Pharmaceutical Research, Vol. 22, No. 8, August 2005 (© 2005)
DOI: 10.1007/s11095-005-5277-5

Research Paper

Distribution and Effect of Water Content on Molecular Mobility in Poly(vinylpyrrolidone) Glasses: A Molecular Dynamics Simulation

Tian-Xiang Xiang[1] and Bradley D. Anderson[1,2]

Received January 25, 2005; accepted April 6, 2005

Purpose. This work explores the distribution of water and its effects on molecular mobilities in poly(vinylpyrrolidone) (PVP) glasses using molecular dynamics (MD) simulation technology.
Methods. PVP glasses containing 0.5% and 10% w/w water and a small amount of ammonia and Phe-Asn-Gly were generated. Physical aging processes and associated structural and dynamic properties were monitored *vs.* time for periods up to 0.1 μs by MD simulation.
Results. Increasing water content from 0.5% to 10% w/w was found to reduce the T_g by about 90 K and increase the rates of volume and enthalpy relaxation. At 0.5% w/w, water molecules are mostly isolated and uniformly distributed while at 10% w/w, water distribution is markedly heterogeneous, with strands of water molecules occupying channels between the polymer chains. At 10% w/w, each water molecule has an average of 2.0 neighboring water molecules. The plasticization effects of water were revealed in diffusion coefficient increases of 3.7-, 7.3-, and 7.6-fold for water, ammonia, and the individual polyvinylpyrrolidone segments, respectively, and in shorter relaxation times (37- to 47-fold) for rotation of polymer segments with an elevation in water content from 0.5% to 10% w/w. Water diffusivity was found to linearly correlate with the number of neighboring water molecules. Rotation of the PVP segments is comprised of a fast wobble motion within a highly restrained cavity and a slow rotation over a wider angular space. Only the slow rotation was shown to be significantly affected by water content.
Conclusions. Water distribution in the PVP glass is highly heterogeneous at 10% w/w water, reflecting the formation of water strands or small clusters rather than complete phase separation. Local enhancement of mobility with increasing water content has been demonstrated using MD simulations.

KEY WORDS: amorphous polymers; diffusion; molecular dynamics simulation; molecular mobility; PVP; solid-state stability; water uptake.

INTRODUCTION

Amorphous materials are widely employed in the pharmaceutical industry as components in capsule and tablet formulations, lyophilized products, and controlled release drug delivery systems. The potential improvement in oral bioavailability of poorly soluble drugs administered in amorphous form, which promotes solubility and dissolution rate (1,2), has led to a resurgence of interest in solid dispersions of amorphous drugs stabilized in amorphous polymers such as poly(vinylpyrrolidone) (PVP), a polymer that is widely used in the drug industry (3,4). Inhibition of crystal nucleation and growth is a prerequisite for the successful development of such amorphous systems (3,5,6). The inhibition of crystallization of amorphous drugs by excipients is often attributed to specific interactions between the drug and excipient and a decreased molecular mobility in amorphous glasses with high glass transition temperatures (5).

Amorphous drugs are not only metastable because of their potential to crystallize, but also generally less stable chemically than their crystalline forms (7,8). Stabilizing peptides and proteins in amorphous solid formulations is a frequent concern in the development of lyophilized products, where poor stability in aqueous solution may have been a factor in the decision to produce a lyophile (9,10). The extent to which a given protein/peptide can be stabilized in the amorphous solid state depends on several interdependent factors (e.g., temperature, residual water, the viscoelastic state of the amorphous solid, chemical nature of the excipients, effective pH, and the potential degradation pathways). Molecular mobility, a property related to several of the above factors, is a primary contributor to the instability of lyophilized proteins and other amorphous drugs, even at temperatures well below the glass transition (11,12). Understanding diffusion mechanisms in amorphous polymers is also imperative for developing polymeric matrices for controlled release applications and for controlling the effects of water vapor transmission through film coatings and packaging materials. Consequently, molecular mobility in amorphous solids has

[1] Department of Pharmaceutical Sciences, College of Pharmacy, University of Kentucky, Lexington, Kentucky 40536, USA.
[2] To whom correspondence should be addressed. (e-mail: bande2@email.uky.edu)

ABBREVIATIONS: ACF, autocorrelation function; DSC, differential scanning calorimetry; ESP, electrostatic potential; MD, molecular dynamics; NMR, nuclear magnetic resonance; PVP, poly(vinylpyrrolidone).

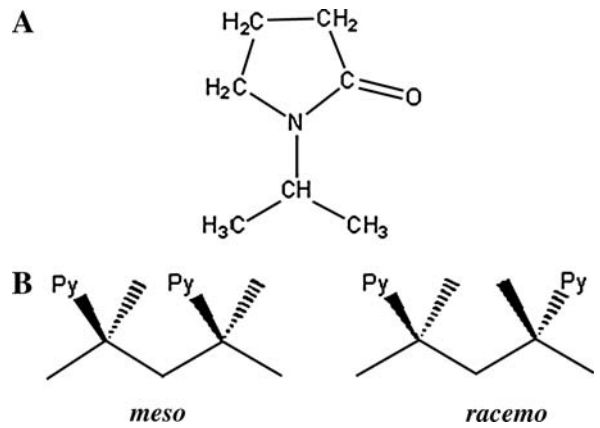

Fig. 1. (A) Chemical structure of a PVP monomer, vinylpyrrolidone (VP). (B) Tacticities (*racemo* and *meso*) of adjacent pairs of monomers in PVP.

been the subject of numerous investigations using various experimental and computational methods such as nuclear magnetic resonance (NMR) (13–15), dielectric relaxation (16–18), differential scanning calorimetry (DSC) (5,11), and molecular dynamics (MD) simulation (19–21).

Water content plays a critical role in protein decomposition in amorphous solids (22–24). However, the precise role played by water is often obscured by the diverse number of possible ways in which it may impact protein stability (e.g., as a nucleophile, as a catalyst for proton transfers, as a solvent, or as a plasticizer) (10,25). Thermomechanical, calorimetric, NMR, and computational studies (18,20,26,27) have shown that water can alter glass transition temperatures (T_g), polymer relaxation times, and the mobilities of dissolved solutes in various polymers. However, the molecular mechanisms responsible for these water-induced changes are poorly understood. For example, it is unclear if water molecules mix in the PVP polymer matrix heterogeneously or in a somewhat ideal manner. Also uncertain are the molecular mechanisms by which water content contributes to increasing solute mobility.

MD simulations have been widely used for the investigation of the structure and dynamics of polymers and other condensed materials (28,29), resulting in significant progress toward understanding glass transition phase behaviors (30–32) and molecular motions accompanying relaxation and diffusion in amorphous polymers (20,21,28,29,33). Recent MD simulations by Karlsson and coworkers (20, 34) at water concentrations up to 5.2% revealed that water is homogeneously distributed in a polar, hydrogen bonding polymer, poly(vinyl alcohol). The primary rate-controlling factor for water diffusion in this hydrophilic polymer is the constraining effect of hydrogen bonds formed between polymeric chain segments. In contrast, water clusters of various sizes were observed in the nonpolar polymer polyethylene, and diffusivity for the water cluster was reported to be one order of magnitude lower than that of a single water molecule (19).

In this study, molecular dynamics simulations have been conducted to explore the distribution and plasticization effects of water in PVP (Fig. 1), a polar but non-hydrogen-bond-donating amorphous polymer. In the glassy state, PVP can significantly inhibit crystallization (35,36) and drug degradation (24,25). PVP can spontaneously absorb a significant amount of water from its environment even at a low humidity, which strongly influences the glass transition, polymer structure, and stability of dissolved proteins (27,37). Systems containing PVP at a chain length comparable to a commercial PVP product were constructed at 0.5% and 10% w/w water including, in addition, small amounts of ammonia and a model tripeptide, Phe-Asn-Gly. The asparagine residue in this peptide can react to yield a cyclic imide followed by hydrolysis or back reaction with ammonia. This system may therefore serve as a prototype for deamidation and covalent aggregate formation of more complex proteins (38,39) in amorphous polymers, which depend on the plasticization effect of water (24,37). Additional MD runs were conducted in water to compare the dynamic properties of the solutes in the PVP glasses with those in water.

COMPUTATIONAL METHODS

Most of the computational detail has been described previously (21). Briefly stated, polymer assemblies containing six PVP chains (each having 40 monomer units), 8–167 water molecules, 8 ammonia molecules, and one Phe-Asn-Gly peptide were built using xLeap in the AMBER 6 program suite (40). The molecular mass for a PVP chain is 4456 Da, which is close to the average molecular mass of 4000 for a commercial PVP product, Kollidon K12 (BASF Co.). Since the CH-N carbon in the PVP monomer (see Fig. 1A) is a chiral center, the PVP structure depends on the distribution of the handedness of successive chiral centers along the polymer backbone (i.e., *racemo* and *meso*). ^{13}C NMR studies for PVP found a slight preference for *racemo* (55%) with an otherwise random distribution throughout the polymer (41). This preference depends slightly on the method of polymer synthesis (42). The sequences of dyads in the PVP chains used in this study were determined from random numbers chosen between 0 and 1.0 (*racemo*, 0.0–0.55; *meso*, 0.55–1.0). Some simulations were also performed in pure water for comparison. The water assemblies were built by soaking 8 ammonia molecules and one Phe-Asn-Gly within a box of 571 water molecules using xLeap.

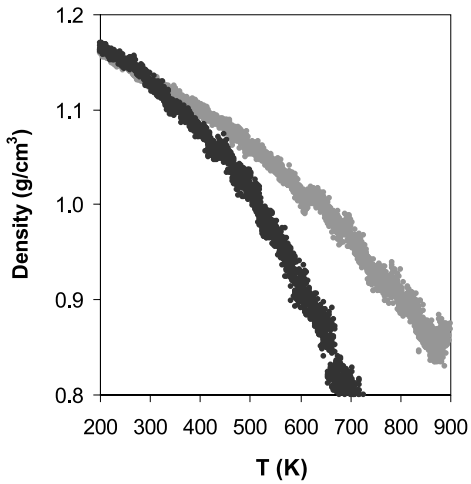

Fig. 2. Density *vs.* temperature diagrams for the PVP systems containing 0.5% (gray) and 10% w/w water (black) at a constant pressure of 1 bar. The cooling rate for both systems was 0.1 K/ps.

The ff99 force field parameters (43) with revised ϕ/ψ dihedral parameters to improve agreement with *ab initio* relative energies of alanine tetrapeptide conformations (44) were used. Partial charges for molecules in water were calculated at the level of HF/6-31G*, which systematically overestimates dipole moments and thereby implicitly includes solvent polarization (45,46). Partial charges for PVP monomer atoms and the solutes were obtained by first calculating the electrostatic potentials (ESPs) of the optimized structures at the level of B3LYP/cc-pVTZ (47,48) using Gaussian 98 (49), which was followed by fitting the ESPs using RESP (50,51) in AMBER 6 to yield sets of point charges. These sets of charges were then scaled by a factor of 1.1 to approximately account for polarization in PVP, which is a polar polymer but less polar than water. This scaling method gave better agreement between calculated and experimental chloroform/water partition coefficients of *N*-methylated nucleic acid bases (52). Separately, we have shown that partial charges for alanine peptides obtained at the level of B3LYP/cc-pVTZ agree with those obtained at the level of HF/6-31G* when adjusted by a scaling factor of 1.2–1.3 (53).

Once constructed, the PVP assemblies were energy minimized (500 iterations each of steepest descent and conjugate gradient) to eliminate possible bad contacts. The

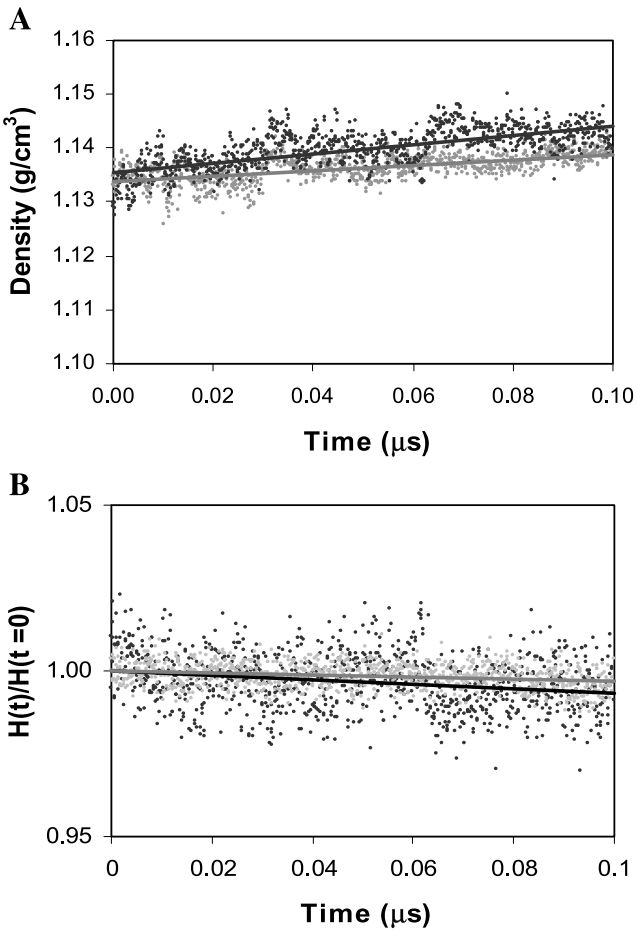

Fig. 3. Density (A) and enthalpy (B) relaxation in simulated PVP glasses containing 0.5% (light) and 10% w/w (dark) water at 298 K and 1 bar.

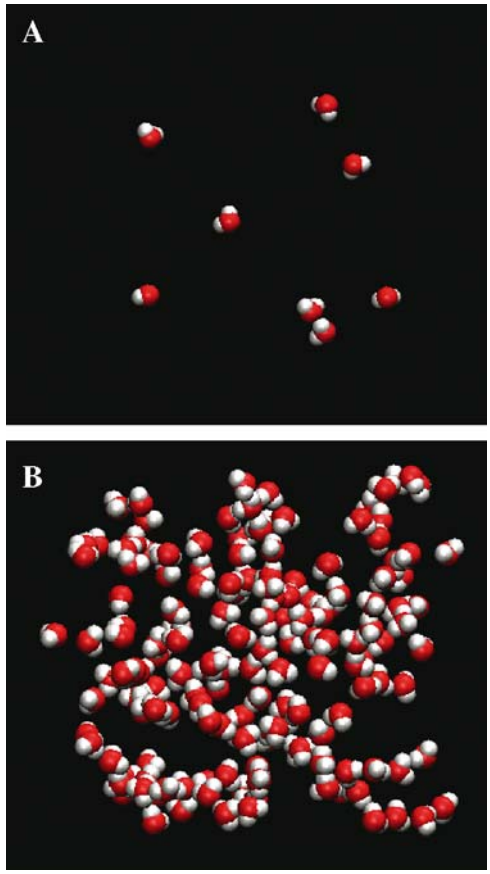

Fig. 4. Spatial distributions of water molecules obtained from two instantaneous structures of the PVP glasses with 0.5% (A) and 10% (B) water by weight.

PVP and water assemblies were then equilibrated at 1 bar and 700–900 K and 298 K, respectively, by dynamic simulations (1–2 ns) subjected to periodic boundary conditions. The minimization and dynamic runs were performed using Sander 7, in which Newton's equations of motion were evolved using the Verlet leapfrog algorithm (54) with a time step of 1–2 fs. The dielectric constant was set at 1.0. Constant temperature and pressure were maintained by coupling to external thermal baths (55). Electrostatic interactions were calculated via the Particle Mesh Ewald method (56) with a cutoff of 9 Å. The SHAKE algorithm was used to constrain all covalent bonds involving hydrogen. The equilibrated PVP systems were then subjected to dynamic runs during which the system was cooled to a final temperature of 200 K at 0.1 K/ps. After the completion of a cooling run, a selected PVP structure corresponding to a certain temperature (i.e., 298 K) from the acquired trajectory file was used as a restarting configuration for a prolonged aging dynamic run (0.1 μs) at the same temperature and pressure to acquire system trajectories at 2- to 4-ps intervals for subsequent calculations. A similar dynamic run was performed in the water system. The *ptraj* and *carnal* programs in Amber 6, the VMD 1.8.2 (57), and computer programs developed in house were utilized to calculate numerically and analyze visually various structural and dynamic properties of the PVP chains and embedded solutes. Calculations were performed on an HP Superdome at the University of Kentucky, an IBM pSeries

690 cluster at the National Center for Supercomputing Applications, University of Illinois at Urbana-Champaign, a Linux/Intel cluster, and four HP and SGI workstations at the Center for Computational Sciences, University of Kentucky, and a PC in the authors' laboratory.

RESULTS

Water-Induced Thermodynamic Changes in Simulated PVP

The PVP systems constructed at 0.5% and 10% w/w water were equilibrated at a high temperature and cooled through the glass transition temperature at a rate of 0.1 K/ps to obtain polymer glasses. The density *vs.* temperature profiles for PVP containing 0.5% and 10% w/w water are presented in Fig. 2. Decreases in slope are evident upon cooling ($-6.0 \times 10^{-4} \rightarrow -3.2 \times 10^{-4}$ g/cm^3 K at 0.5% w/w water and $-10.8 \times 10^{-4} \rightarrow -4.5 \times 10^{-4}$ g/cm^3 K at 10% w/w water) from which estimates of T_g can be obtained. The slope changes more abruptly at a higher water content. T_g values estimated from the changes in slope at the lower and higher ranges of temperature are 560 ± 15 K and 470 ± 10 K at 0.5 and 10% w/w water content, respectively.

The PVP glasses formed after the cooling processes, which are not at equilibrium states, were then subjected to long simulations (up to 0.1 μs) at 298 K and 1 bar to evaluate the aging of thermodynamic properties such as density and enthalpy ($\Delta H° = \Delta E° + p\Delta V°$) of the PVP glasses. Gradual changes in density and enthalpy are visible in Fig. 3 despite large thermal fluctuations. Relaxation times for these processes would be desirable to estimate, but this requires knowledge of the equilibrium values for these properties. Considering first the density, the initial densities for the simulated PVP glasses are about 10% lower than the experimental values (ca. 1.25 g/cm^3) for commercial PVP glasses because of the rapid cooling in the simulation (3). As a first approximation, we assume that the experimental density reflects a pseudo-equilibrium value and the relaxation processes are first order. A least-squares regression analysis of the density data in Fig. 3 on the basis of these assumptions yields relaxation times (i.e., inverses of the first-order rate constants) of 2.47 ± 0.02 and 1.28 ± 0.03 μs at 0.5% and 10% w/w water, respectively. The simulated glasses containing 0.5% and 10% w/w water had initial enthalpies of 4200 and 2300 kcal/mol, respectively. Over the 0.1-μs simulation, the system enthalpies decreased by (0.34 ± 0.04) % and (0.71 ± 0.09) %, respectively.

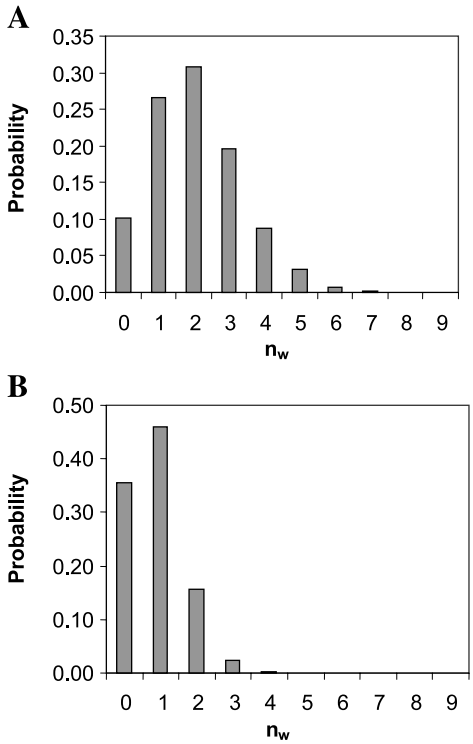

Fig. 5. Probability distributions for the number of water molecules (n_w) surrounding a given water molecule (A) or carbonyl oxygen atom (B) in simulated PVP glass with 10% water by weight.

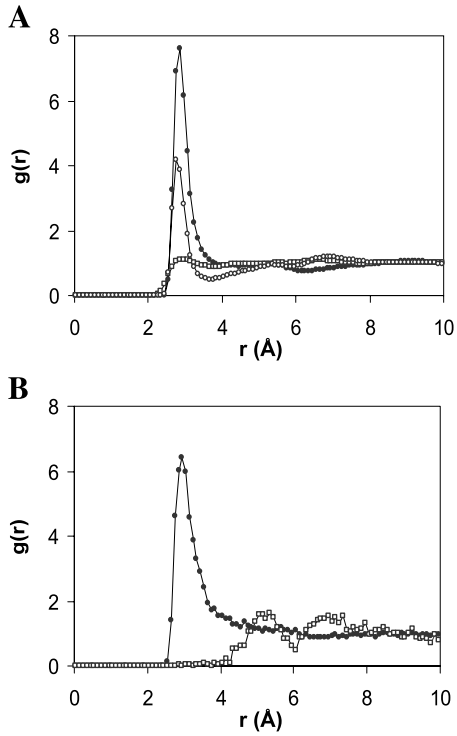

Fig. 6. (A) Radial distribution functions, g(r), between the oxygen atoms in water molecules and oxygen atoms in other water molecules (solid circles), carbonyl oxygen atoms (open circles) or hydrogen atoms (open squares) of all methylenes in PVP containing 10% w/w water. (B) Radial distribution functions, g(r), for the nitrogen atoms in ammonia molecules (solid circles) or the glycine amide nitrogen atom in the tripeptide (open circles) with respect to water molecules in PVP containing 10% w/w water.

Water Distribution and Cluster Formation in Simulated PVP

Snapshots of the spatial distribution of water in the simulated PVP are shown in Fig. 4. At 0.5% w/w water (Fig. 4A), the water molecules are mostly isolated from each other and appear to be distributed uniformly throughout the polymer. On the other hand, at a concentration of 10% w/w, water's distribution is markedly heterogeneous, with clusters or strands of water molecules occupying channels between the polymer chains.

The state of water in PVP at 10% w/w was characterized quantitatively by the number (n_w) of water molecules within a certain distance (3.4 Å in this study) of another water molecule or a given atom of interest (e.g., PVP carbonyl oxygen). A water molecule was considered as being within the solvation shell if any atom of the water was within 3.4 Å. The probability distribution for n_w surrounding a water molecule, averaged over the entire simulation time (0.1 μs), is shown in Fig. 5A. The average number of water neighbors for a water molecule in the PVP was found to be 2.0 with an apparent standard deviation of 2.1 indicating a broad distribution. Structural relaxation alters water's distribution as n_w increased from 1.9 to 2.2 over 0.1 μs simulation (data not shown).

The probability distribution for the number of water molecules (n_w) surrounding a carbonyl oxygen atom in the simulated PVP at 10% w/w water is shown in the upper panel of Fig. 5. The average number of water neighbors per carbonyl oxygen atom was found to be 0.86 with a wide standard deviation of 1.2. About 35.5%, 46.0%, 15.7%, and 2.5% of the carbonyl oxygen atoms in PVP had 0, 1, 2, and 3 water molecules, respectively, within 3.4 Å.

The distribution of water in PVP at 10% w/w was further explored by generating radial distribution functions g(r) for the oxygen atoms in water molecules with respect to: (a) oxygen atoms in other water molecules, (b) oxygen atoms in the carbonyl groups of PVP, and (c) hydrogen atoms in nonpolar methylene groups of PVP. The results are presented in Fig. 6A. The lower panel shows similar curves for ammonia and the glycine amide nitrogen atom of the tripeptide with respect to water. Distinct peaks are evident near the first-shell distance for water and the polar carbonyl groups in PVP with respect to other water molecules, suggesting there is a higher probability for a water molecule to have either a water molecule or a carbonyl group adjacent to it in PVP than predicted from a uniform statistical distribution. A similar result was also found for the radial distribution of ammonia with respect to water (Fig. 6B). The g(r) distribution for water with respect to the nonpolar PVP methylene groups is roughly uniform beyond the close-contact distance (2.6 Å) indicating no preferential solvation by water. Similarly, the g(r) distribution for oxygen atoms in water molecules with respect to the glycine amide nitrogen atom in the tripeptide (Fig. 6B) demonstrates a low probability for finding water in the first-solvation shell near the glycine amide nitrogen.

Molecular Diffusivity in Simulated PVP

Molecular diffusivity in the simulated PVP was assessed by monitoring the mean-squared displacements, $\langle|r(t) - r(0)|^2\rangle$ ($\langle r^2\rangle$), for water, ammonia, Phe-Asn-Gly, and individual vinylpyrrolidone (VP) segments over time (t) at 0.5 and 10% w/w water. The results are presented in Fig. 7 as log–log plots. The diffusivity of PVP chains as a whole would be expected to be extremely slow. However, pseudo-diffusional motions of local VP segments, although constrained by covalent bonds with adjacent VP segments, may exist over a short time. These motions may affect the rate of free-volume redistribution, a key factor for solute diffusion in polymers (58). Apparent diffusion coefficients for water, ammonia, and

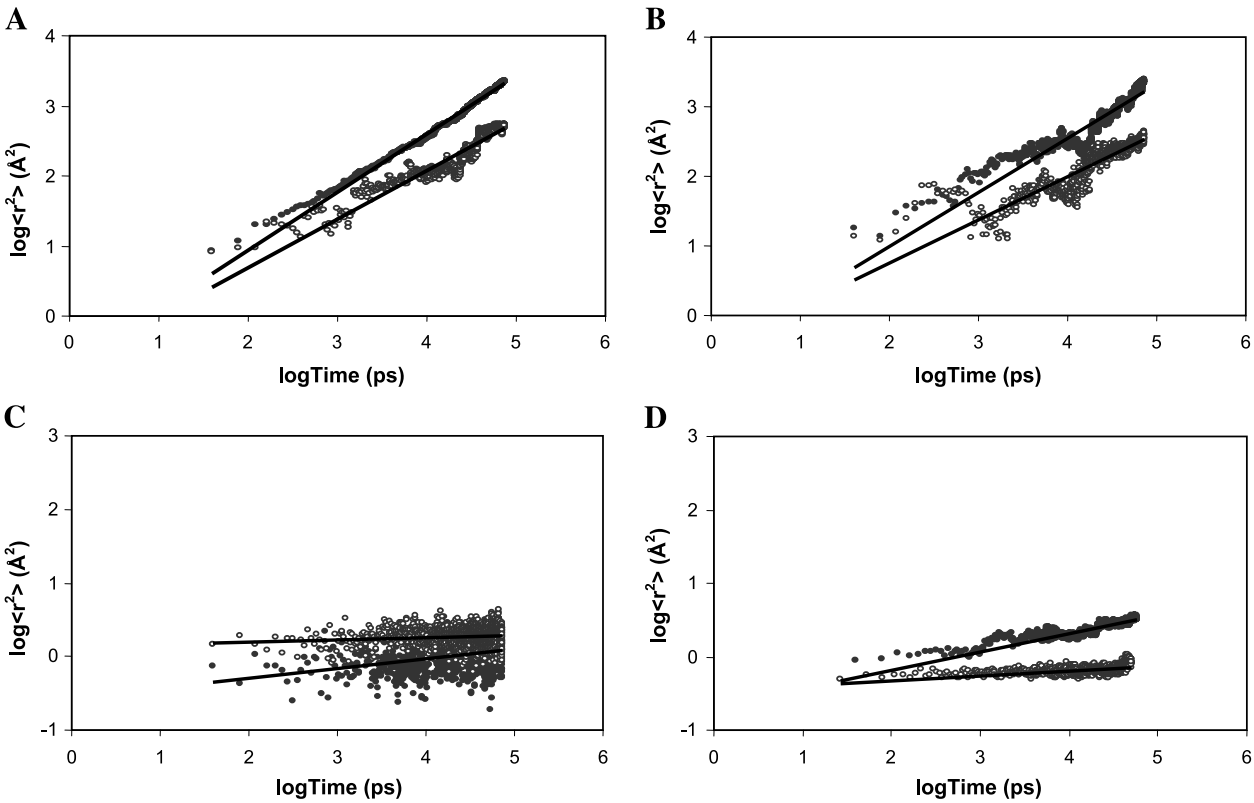

Fig. 7. Log–log plots of the mean-squared displacements, r^2, *vs.* time for (A) water, (B) ammonia, (C) Phe-Asn-Gly, and (D) individual VP-segments in the simulated PVP glasses at 298 K. Open circles, 0.5% w/w water; and solid circles, 10% w/w water. The lines are the least-squares fits.

Table I. Structural and Dynamic Properties in Simulated PVP Glasses at 298 K and Two Different Water Concentrations

	Water content %w/w	
Properties	0.5	10.0
T_g (K)	560 ± 15	470 ± 10
C_1		
C–C	0.040 ± 0.000	0.042 ± 0.001
C=O	0.110 ± 0.000	0.111 ± 0.001
τ (μs)		
C–C	$(3.3 \pm 0.4) \times 10^{3}$	$(7.0 \pm 0.4) \times 10^{1}$
C=O	$(4.5 \pm 0.4) \times 10^{2}$	$(1.2 \pm 0.1) \times 10^{1}$
D (cm^2/s)		
Water	$(1.3 \pm 0.0) \times 10^{-7}$	$(4.8 \pm 0.0) \times 10^{-7}$
NH_3	$(7.0 \pm 0.1) \times 10^{-8}$	$(5.1 \pm 0.0) \times 10^{-7}$
VP segment	$(6.0 \pm 0.2) \times 10^{-11}$	$(4.6 \pm 0.0) \times 10^{-10}$

the VP segment were calculated from the slopes of linear fits of the $<r^2>$ *vs.* t curves ($<r^2> = 6Dt$), as reported in Table I. Because of its size, the tripeptide was found to be virtually frozen in its original position during the entire simulation period.

To evaluate the effects of neighboring water molecules on water diffusivity, we sorted all the water molecules in the PVP glasses at 0.5% and 10% w/w water in terms of the number of surrounding (first-shell) water molecules they possessed (averaged over the entire simulation run) and calculated the respective diffusion coefficients for the sorted water molecules. The results are presented in Fig. 8. A linear least-squares fit yields a positive increase in diffusivity of $(2.6 \pm 0.3) \times 10^{-7}$ cm^2/s ($r^2 = 0.99$) per neighboring water molecule.

Polymer Segment Relaxation Rates in Simulated PVP

Another important component of polymer mobility is the rotational relaxation of PVP segments, which can be evaluated by the autocorrelation function (ACF) for selected atomic bonds on the PVP backbone (e.g., C–C) and side chains (e.g., C=O). The ACF is defined as

$$C(t) = \frac{\langle \vec{m}(0) \cdot \vec{m}(t) \rangle}{\langle m^2(0) \rangle} \qquad (1)$$

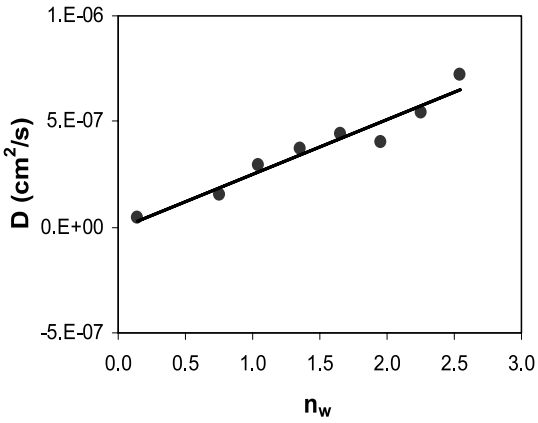

Fig. 8. Correlation between the diffusion coefficient D for water and the number of first-shell water molecules in the PVP glass containing 0.5% and 10% w/w water.

where $m(t)$ is the vector connecting the atoms of interest and the brackets indicate averages over multiple starting points (t = 0) along a molecular trajectory. The results of this calculation averaged over all of the PVP chains are presented in Fig. 9. In general, the ACFs exhibited an initial fast decay within 2 ps followed by a slow decline that was incomplete over the 0.1-μs time scale. The first-decay component reflects wobble motions of the PVP segments within a local cavity, the extent of which can be characterized by c_1, the depth of this initial decay prior to the onset of a second slower decline. The results are summarized in Table I.

The second slower decay covers a wider rotational space and, as such, requires some cooperative motions of neighboring polymer chains. Based on this concept, which was first proposed by Glarum (59) in the so-called defect relaxation model, one can describe the second slower decay by the Kohlrausch-Williams-Watts (KWW) function (60–62):

$$f_{KWW}(t) = \exp\left[-(t/\tau)^{\beta}\right] \qquad (2)$$

where τ and β are respectively a central relaxation time and a stretching parameter between 0 and 1. The second decays of the ACFs in Fig. 9 were fitted with this equation which was modified to include the pre-exponential factor, c_1. Although least-squares fits resulted in excellent statistics ($r^2 > 0.99$), the regression results are at best approximations of the long-term relaxation behavior because of the lack of completion of the slow decay over the 0.1-μs simulation time. This results in a high correlation between the τ and β values, such that a small change in β would lead to a large change in τ. Since β for the four curves in Fig. 9 varies over a range of 0.30–0.47 with an average value of 0.39, the same curves were refit with a fixed β value of 0.39. The parameter values generated at the fixed β are presented in Table I. A similar β value (0.36) was reported for dipolar relaxation in glassy polyethylene, a structurally simpler and more flexible polymer (28).

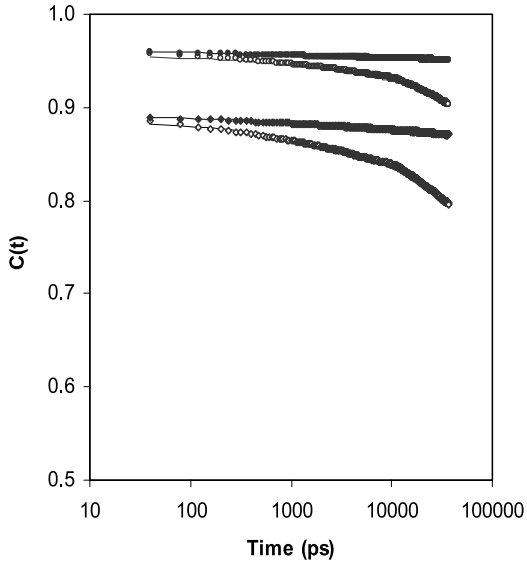

Fig. 9. Averaged autocorrelation functions for rotational relaxation of backbone alkyl bonds (circles) and side-chain carbonyl bonds (diamonds) in the PVP systems containing 0.5% (solid) and 10% w/w water (open). The curves are least-squared fits obtained using the modified KWW function.

DISCUSSION

Glasses are often prepared by cooling an initially melted material. If crystallization does not occur during cooling, then a "glass transition" occurs, which has been described as the range of temperatures over which the system "falls out of equilibrium" (63). The glass transition temperature therefore depends on the time scale over which cooling occurs. The rate of cooling in the present simulations (0.1 K/ps) was considerably faster than that typically employed experimentally. The approximate glass transition temperatures estimated in these simulations are ca. 100 K higher than experimental T_g values for PVP (K 90) containing the same amounts of water but obtained at much slower heating/cooling rates of 0.3–0.7 K/s (11,27). Similar differences were reported in computer simulations of other polymers and silica glasses (31,64). The faster cooling rate employed in the simulations is considered to be the main cause for the discrepancy, although other factors such as differences in polymer chain lengths, the presence of small amounts of residual monomer, and branching of PVP chains may also have affected the experimental values (65). The ~90 K reduction in the glass transition temperature (T_g) when the water content increased from 0.5% to 10% w/w resembles that obtained experimentally (ca. 100 K) (26,27).

The PVP glasses generated in the cooling processes were far from thermodynamic equilibrium. Their physical properties such as density and enthalpy were found to drift slowly and monotonically during subsequent MD simulations at 298 K and 1 bar, as shown in Fig. 3. The relaxation rates for both the system density and the system enthalpy were about twofold larger at 10% w/w water than at 0.5% w/w water. The faster density and enthalpy relaxation at the higher water content can be attributed to higher mobilities of the various components in the polymer also found in this study.

An understanding of the plasticization effects of water on the structure and dynamics of PVP initially requires knowledge of water's distribution in the polymer. The snapshots of water molecules in the simulated PVP as shown in Fig. 4 indicate that water molecules are mostly isolated from each other at 0.5% w/w water while water's distribution is markedly heterogeneous at the higher water content (10% w/w), with clusters or strands of water molecules occupying channels between the polymer chains. Water distribution in PVP was further described in terms of the number (n_w) of water molecules within 3.4 Å of a target water molecule or PVP carbonyl atom. The results in Fig. 5 indicate that a water molecule is, on the average, in close contact with 2.0 other water molecules at a water content of 10% w/w. A linear H-bonded chain of water molecules would have two nearest neighbor H-bonded water molecules for each internal water molecule in the chain.

Also evident in Fig. 5 is that 64% of the carbonyl oxygen atoms in PVP are within a distance of 3.4 Å from the oxygen atom of at least one water molecule. Since the number of PVP monomer residues (240) is 44% higher than the number of water molecules available (167), it is likely that most of the available water molecules are in close contact with PVP carbonyl groups. This appears to be consistent with FTIR spectra in the region of 3600–3200 cm^{-1}, where three absorption bands have been attributed to sorbed water in PVP (66). The absence of bands for unbound hydroxyl groups was taken as evidence that all the protons of water molecules are either H-bonded to the polymer or to other molecules of absorbed water. Lebedeva *et al.* also concluded from FTIR spectra that, at low water content, water molecules hydrogen bond to the PVP carbonyl groups (66).

At 10% w/w water, there is a twofold higher probability for water to hydrogen bond with another water molecule than with a PVP carbonyl group even though the number of monomer residues exceeds the number of water molecules available. Similar results were also reported in PVA (67). This may be rationalized by the fact that a carbonyl oxygen atom has two electron pairs capable of forming two hydrogen bonds with water while water can form four hydrogen bonds with neighboring water molecules. A linear water strand in which each water molecule is hydrogen bonded to a PVP carbonyl residue also yields a 2:1 ratio of water–water to water–carbonyl hydrogen bonds.

Experimental evidence based on T_g data for PVP *versus* water content (26,27) suggests apparently ideal mixing behavior at water contents up to 10% water by weight while deviations from ideality occur above 10% w/w water. One interesting scenario to consider is that of complete phase separation of water from the PVP glass as suggested by Franks (68). In the present simulations at 10% w/w water, the value of 2.0 for the number of neighboring water molecules within 3.4 Å of a reference water molecule in PVP was found to be far below the value for n_w (8.9) obtained in bulk water using the same distance criteria. Thus, there is no evidence in the MD simulation for phase separation at 10% water content. Hamaura and Newton also ruled out complete phase separation below a weight fraction of water of 0.47 based on the absence of a melting peak for water in DSC experiments (26).

The diffusion coefficients obtained for water in the simulated PVP, 1.3–4.8 $\times$ 10^{-7} cm^2/s, appear to slightly exceed or lie near the upper end of the range of reported values (12,69,70). This may be attributed to: (1) the lower densities (ca. 10%) of the simulated PVP due to the faster cooling rate (0.1 K/ps); and (2) the short length of time (0.1 μs) during which the diffusion coefficients were calculated. The latter argument is supported by the fact that solute diffusion in amorphous polymers and other similar systems (e.g., lipid membranes) may exhibit two or more diffusion coefficients differing by one to three orders of magnitude depending on the time scales of measurement methods such as NMR, fluorescence and neutron scattering (71,72). The short simulation length also caused anomalous non-Einsteinian diffusion behavior as demonstrated by curvature in plots of log r^2 *vs.* log t with slopes <1 (Fig. 7). Estimates of the slopes for water, ammonia, and the VP segments in simulated PVP containing 0.5% w/w water were 0.70, 0.62, and 0.07, respectively, increasing to 0.83, 0.77, and 0.25 when the water content was elevated from 0.5% to 10% by weight. Evidently, the larger solute (VP) exhibits greater deviation in its diffusion from the Einstein relation. Anomalous diffusion behaviors have also been found in other polymers [e.g., oxygen and helium in polyisobutylene (73); helium in polypropylene (33)], although over a shorter time scale of 1 ns. In the present case, anomalous diffusion behavior persisted well over 100 ns, especially for the larger species, presumably owing to the more dense packing in the PVP

glass [1.13 g/cm^3, compared with 0.93 g/cm^3 for polypropylene in the study by Boshoff *et al.* (33)].

Reaction rates in amorphous glasses may be rate limited by the relative diffusion coefficients of the reactants, which is strongly affected by moisture content (22,37,39). The diffusion coefficients for water, ammonia, and the VP segment were found in this study to be increased by 3.7-, 7.3-, and 7.6-fold, respectively, when the water content was elevated from 0.5% to 10% w/w. These increases are consistent with the general trend of increasing diffusivity with increasing water content observed experimentally (12,70,74). In particular, Oksanen and Zografi (12) found an increase in water's diffusion coefficient of 3.1-fold when the water content was increased from near zero to 10% w/w. Also, the diffusion coefficients obtained for water in the simulated PVP, 1.3–4.8 $\times$ 10^{-7} cm^2/s, are about two orders of magnitude smaller than the diffusivity (3.4 $\times$ 10^{-5} cm^2/s) in pure water (21).

Mechanistically, increased solute diffusivity in a PVP glass containing a higher water concentration (i.e., 10% w/w) may arise from a global change in the polymer structure (e.g., a change in the free-volume) or from a local change due to the presence of an increased number of water molecules in close proximity to the diffusing solute. To test the latter hypothesis, we calculated the diffusion coefficients for water molecules as a function of their n_w values. The positive slope (2.6 $\times$ 10^{-7} cm^2/s per neighboring water molecule) in Fig. 8 suggests that, indeed, water molecules with a higher diffusivity tend to be those surrounded by more water molecules, and that water's plasticization effect on solute diffusivity is at least partly a local phenomenon.

The effects of water on polymer chain dynamics were further evaluated by generating ACFs for rotational relaxation of various PVP segments of interest. As illustrated in Fig. 9, the ACFs exhibited an initial fast decay followed by a slow decline. The initial rapid decay was much steeper for the side-chain C=O groups than for the backbone C–C groups. Clearly, the polymer side chains can wobble over a wider angular space than the backbones. Surprisingly, water content appeared not to affect c_1 to a large degree, suggesting that the free volume surrounding the PVP segments available for these wobble motions does not increase with water content. This is also in line with the finding that water content does not greatly affect the overall density of the polymer glasses (see Fig. 2).

The relaxation time, τ, for the slower second decay, was found to depend strongly on the water content. As indicated in Table I, the τ values for the C=O groups decreased from 440 to 12 μs and those for the –C–C– backbone decreased from 3300 to 70 μs when the water content in the PVP glass increased from 0.5% to 10% w/w, representing increases of 37- and 47-fold, respectively. Oksanen and Zografi (12) utilized ^{13}C solid-state NMR to examine the effect of absorbed water on three PVP resonances at 2°C and 50 MHz. All three resonances indicated a dramatic increase in mobility with an increase in water content from 0% to 10% (by weight), though the magnitude of the change (~3-fold) was less than that in the present simulations. Taken together, the above results thus suggest that an increase in water content greatly increases the mobility of the polymer chains and thereby the rate of free-volume redistribution while exerting only a minor effect on the overall amount of free volume in the polymer. These findings appear to refute the first hypothesis proposed above that a global change in polymer structure such as an increase in free-volume is the primary factor accounting for the increased solute diffusivity at higher water content.

CONCLUSIONS

An increase from 0.5% to 10% w/w water was found to reduce the glass transition temperature of the simulated PVP by 90 K. At 10% w/w, water's distribution is heterogeneous and dominated by water strands or clusters with the number of first-shell waters (n_w) averaging roughly 2 but varying from 0 to 6. These clusters are much smaller than those observed in bulk water, suggesting that there is no phase separation at 10% w/w water. The higher water content promotes the relaxation (aging) rates of the thermodynamic properties of the initially prepared PVP glasses such as the volume and enthalpy. The plasticization effects of water are also reflected in higher diffusivities (3.7- to 7.6-fold) for the small molecule solutes and polymer segments and shorter relaxation times (37- to 47-fold) for rotation of the polymer segments. The diffusivity increases were found to correlate closely with the number of first-shell water molecules. Rotation of the PVP segments is comprised of a fast wobble motion within a highly restrained cavity and a slow rotation over a wider angular space. The fast wobble motion at the water content of 0.5% and 10% w/w as measured by c_1 (see Table I) suggests a similar amount of free-volume available for segmental rotation at these two water concentrations. Thus, models based on the concept of instantaneous redistribution of free volume (75) are unable to account for these substantial increases in solute diffusivity with water content in PVP. Rather, the effects of the translational and rotational mobilities of the polymer chains and other species (e.g., water) to solute diffusion must be considered, as emphasized in a dynamic free-volume theory proposed by Xiang (76). A future study will further explore the multiple roles played by water molecules surrounding a diffusing solute in assisting its diffusion including: (1) promotion of free-volume redistribution, (2) participation in local cooperative rotation by position exchange with the diffusing solute, and (3) facilitation of the movement of a diffusing molecule along a particular coordinate via strong electrostatic interactions or hydrogen-bond bridging.

ACKNOWLEDGMENTS

This work was partially supported by a grant from the National Science Foundation, the Industry/University Cooperative Research Centers for Pharmaceutical Processing. The use of the computer resources at the Institute for High Performance Computing and the Center for Computational Sciences, University of Kentucky, is also acknowledged. The authors also appreciate the advice given by many members of the Amber and VMD discussion groups.

REFERENCES

1. J. L. Ford. The current status of solid dispersions. *Pharm. Acta Helv.* **61**:69–88 (1986).

2. B. C. Hancock and M. Parks. What is the true solubility advantage of amorphous pharmaceuticals? *Pharm. Res.* **17**:397–404 (2000).
3. K. Khougaz and S.-D. Clas. Crystallization inhibition in solid dispersion of MK-0591 and poly(vinylpyrrolidone) polymers. *J. Pharm. Sci.* **89**:1325–1334 (2000).
4. P. Gupta, V. K. IKakumanu, and A. K. Bansal. Stability and solubility of celecoxib-PVP amorphous dispersions: a molecular perspective. *Pharm. Res.* **21**:1762–1769 (2004).
5. Y. Aso, S. Yoshioka, and S. Kojima. Molecular mobility-based estimation of the crystallization rates of amorphous nifedipine and phenobarbital in poly(vinylpyrrolidone) solid dispersions. *J. Pharm. Sci.* **93**:384–391 (2004).
6. N. Rodriguez-Hornedo and D. Murphy. Significance of controlling crystallization mechanism and kinetics in pharmaceutical systems. *J. Pharm. Sci.* **88**:651–660 (1999).
7. S. R. Byrn, R. R. Pfeiffer, and J. G. Stowell. *Solid-State Chemistry of Drugs*, SSCI, Inc., West Lafayette, IN, 1999.
8. S. R. Byrn, W. Xu, and A. W. Newman. Chemical reactivity in solid-state pharmaceuticals: formulation implications. *Adv. Drug Deliv. Rev.* **48**:115–136 (2001).
9. J. E. Carpenter, M. J. Pikal, B. S. Chang, and T. W. Randolph. Rational design of stable lyophilized protein formulations: some practical advice. *Pharm. Res.* **14**:969–975 (1997).
10. M. J. Hageman. Water sorption and solid state stability of proteins. In T. J. Ahern and M. C. Manning (eds.), *Stability of Protein Pharmaceuticals: Chemical and Physical Pathways of Protein Degradation*, Plenum, New York, 1992.
11. B. C. Hancock, S. L. Shamblin, and G. Zografi. Molecular mobility of amorphous pharmaceutical solids below their glass transition temperatures. *Pharm. Res.* **12**:799–806 (1995).
12. C. A. Oksanen and G. Zografi. Molecular mobility in mixtures of absorbed water and solid poly(vinylpyrrolidone). *Pharm. Res.* **10**:791–799 (1993).
13. S. Yoshioka, Y. Aso, K. Izutsu, and T. Terao. Stability of β-galactosidase, a model protein drug, is related to water mobility as measured by ^{17}O nuclear magnetic resonance (NMR). *Pharm. Res.* **10**:103–108 (1993).
14. S. Yoshioka, Y. Aso, T. Otsuka, and S. Kojima. Water mobility in poly(ethylene glycol)-, poly(vinylpyrrolidone)-, and gelatin-water systems, as indicated by dielectric relaxation times, spin-lattice relaxation time, and water activity. *J. Pharm. Sci.* **84**:1072–1077 (1995).
15. S. Yoshioka, Y. Aso, S. Kojima, S. Sakurai, T. Fujiwara, and H. Akutsu. Molecular mobility of protein in lyophilized formulations linked to the molecular mobility of polymer excipients, as determined by high resolution ^{13}C solid-state NMR. *Pharm. Res.* **16**:1621–1625 (1999).
16. S. Yoshioka, Y. Aso, and S. Kojima. The effect of excipients on the molecular mobility of lyophilized formulations, as measured by glass transition temperature and NMR relaxation-based critical mobility temperature. *Pharm. Res.* **16**:135–140 (1999).
17. S. Bone. Time-domain reflectrometry studies of water binding and structural flexibility in chymotrypsin. *Biochim. Biophys. Acta* **916**:128–134 (1987).
18. S. P. Duddu and T. D. Sokoloski. Dielectric analysis in the characterization of amorphous pharmaceutical solids. 1. Molecular mobility in poly(vinylpyrrolidone)-water systems in the glassy state. *J. Pharm. Sci.* **84**:773–776 (1995).
19. M. Fukuda and S. Kuwajima. Molecular-dynamics simulation of moisture diffusion in polyethylene beyond 10 ns duration. *J. Chem. Phys.* **107**:2149–2159 (1997).
20. G. E. Karlsson, U. W. Gedde, and M. S. Hedenqvist. Molecular dynamics simulation of oxygen diffusion in dry and water-containing poly(vinyl alcohol). *Polymer* **45**:3893–3900 (2004).
21. T.-X. Xiang and B. D. Anderson. A molecular dynamics simulation of reactant mobility in an amorphous formulation of a peptide in poly(vinylpyrrolidone). *J. Pharm. Sci.* **93**:855–876 (2004).
22. L. N. Bell, M. J. Hageman, and J. M. Bauer. Impact of moisture on thermally induced denaturation and decomposition of lyophilized bovine somatotropin. *Biopolymers* **35**:201–209 (1995).
23. L. N. Bell, M. J. Hageman, and L. M. Muraoka. Thermally induced denaturation of lyophilized bovine somatotropin and lysozyme as impacted by moisture and excipients. *J. Pharm. Sci.* **84**:707–712 (1995).
24. M. C. Lai, M. J. Hageman, R. L. Schowen, R. T. Borchardt, B. B. Laird, and E. M. Topp. Chemical stability of peptides in polymers. 2. Discriminating between solvent and plasticizing effects of water on peptide deamidation in poly(vinyl pyrrolidone). *J. Pharm. Sci.* **88**:1081–1089 (1999).
25. L. N. Bell and M. J. Hageman. Differentiating between the effects of water activity and glass transition dependent mobility on a solid state chemical reaction: aspartame degradation. *J. Agric. Food Chem.* **40**:873–879 (1994).
26. T. Hamaura and J. M. Newton. Interaction between water and poly(vinylpyrrolidone) containing polyethylene glycol. *J. Pharm. Sci.* **88**:1228–1233 (1999).
27. B. C. Hancock and G. Zografi. The relationship between the glass transition temperature and the water content of amorphous pharmaceutical solids. *Pharm. Res.* **11**:471–477 (1994).
28. R. K. Bharadwaj and R. H. Boyd. Effect of pressure on conformational dynamics in polyethylene: a molecular dynamics simulation study. *Macromolecules* **33**:5897–5905 (2000).
29. O. Hahn, D. A. Mooney, F. Muller-Plathe, and K. Kremer. A new mechanism for penetrant diffusion in amorphous polymers: molecular dynamics simulations for phenol diffusion in bisphenol-A-polycarbonate. *J. Chem. Phys.* **111**:6061–6068 (1999).
30. B. F. Abu-Sharkh. Glass transition temperature of poly(vinyl-chloride) from molecular dynamics simulation: Explicit atom model *versus* rigid CH_2 and CHCl groups model. *Comput. Theor. Polymer Sci.* **11**:29–34 (2001).
31. S. U. Boyd and R. H. Boyd. Chain dynamics and relaxation in amorphous poly(ethylene terephthalate): a molecular dynamics simulation study. *Macromolecules* **34**:7219–7229 (2001).
32. E. Tocci, D. Hofmann, D. Paul, N. Russo, and E. Drioli. A molecular simulation study on gas diffusion in a dense poly (ether-ether-ketone) membrane. *Polymer* **42**:521–533 (2001).
33. J. H. D. Boshoff, R. F. Lobo, and N. J. Wagner. Influence of polymer motion, topology and simulation size on penetrant diffusion in amorphous, glassy polymers: diffusion of helium in polypropylene. *Macromolecules* **34**:6107–6116 (2001).
34. G. E. Karlsson, T. S. Johansson, U. W. Gedde, and M. S. Hedenqvist. Physical properties of dense amorphous poly(vinyl alcohol) as revealed by molecular dynamics simulation. *J. Macromol. Sci., Phys.* **B41**:185–206 (2002).
35. A. P. Simonelli, S. C. Mehta, and W. I. Higuchi. Inhibition of sulfathiazole crystal growth by polyvinylpyrrolidone. *J. Pharm. Sci.* **59**:633–638 (1970).
36. H. Sekikawa, M. Nakano, and T. Arita. Inhibitory effect of polyvinylpyrrolidone on the crystallization of drugs. *Chem. Pharm. Bull.* **26**:118–126 (1978).
37. M. Lai, M. J. Hageman, R. L. Schowen, and E. M. Topp. Chemical stability of peptides in polymers. 1. Effect of water on peptide deamidation in poly(vinyl alcohol) and poly(vinylpyrrolidone) matrices. *J. Pharm. Sci.* **10**:1073–1080 (1999).
38. R. G. Strickley and B. D. Anderson. Solid-state stability of human insulin I. Mechanism and the effect of water on the kinetics of degradation in lyophiles from pH 2-5 solutions. *Pharm. Res.* **13**:1142–1153 (1996).
39. R. G. Strickley and B. D. Anderson. Solid-state stability of human insulin II. Effect of water on reactive intermediate partitioning in lyophiles from pH 2-5 solutions-stabilization against covalent dimer formation. *J. Pharm. Sci.* **86**:645–653 (1997).
40. D. A. Case. AMBER 6, University of California, San Francisco, 1999.
41. H. N. Cheng, T. E. Smith, and D. M. Vitus. Tacticity of poly(N-vinylpyrrolidinone). *J. Polym. Sci., Polym. Lett. Ed.* **19**:29, 1981 (1981).
42. J. R. Ebdon, T. N. Huckerby, and E. Senogles. The influence of polymerization conditions on the tacticity of poly(N-vinyl-2-pyrrolidone). *Polymer* **24**:339–343 (1983).
43. J. M. Wang, P. Cieplak, and P. A. Kollman. How well does a restrained electrostatic potential (RESP) model perform in calculation conformational energies of organic and biological molecules? *J. Comput. Chem.* **12**:1049–1074 (2000).

44. C. Simmerling, B. Strockbine, and A. E. Roitberg. All-atom structure prediction and folding simulations of a stable protein. *J. Am. Chem. Soc.* **124**:11258–11259 (2002).
45. W. D. Cornell, P. Cieplak, C. I. Bayly, I. R. Gould, K. M. Merz, D. M. Ferguson, D. C. Spellmeyer, T. Fox, J. W. Caldwell, and P. A. Kollman. A second generation force field for the simulation of proteins, nucleic acids, and organic molecules. *J. Am. Chem. Soc.* **117**:5179–5197 (1995).
46. Y. Duan, C. Wu, S. Chowdhury, M. C. Lee, G. Xiong, W. Zhang, R. Yang, P. Cieplak, R. Luo, T. Lee, J. Caldwell, J. Wang, and P. Kollman. A point-charge force field for molecular mechanics simulations of proteins based on condensed-phase quantum mechanical calculations. *J. Comp. Chem.* **24**:1999–2012 (2003).
47. A. D. Becke. Density-functional thermochemistry. III. The role of exact exchange. *J. Chem. Phys.* **98**:5648–5652 (1993).
48. T. H. Dunning Jr. Gaussian basis sets for use in correlated molecular calculations. I. The atoms boron through neon and hydrogen. *J. Chem. Phys.* **90**:1007–1023 (1989).
49. M. J. Frisch, G. W. Trucks, H. B. Schlegel, G. E. Scuseria, M. A. Robb, J. R. Cheeseman, V. G. Zakrzewski, J. A. Montgomery Jr., R. E. Stratmann, J. C. Burant, S. Dapprich, J. M. Millam, A. D. Daniels, K. N. Kudin, M. C. Strain, O. Farkas, J. Tomasi, V. Barone, M. Cossi, R. Cammi, B. Mennucci, C. Pomelli, C. Adamo, S. Clifford, J. Ochterski, G. A. Petersson, P. Y. Ayala, Q. Cui, K. Morokuma, D. K. Malick, A. D. Rabuck, K. Raghavachari, J. B. Foresman, J. Cioslowski, J. V. Ortiz, A. G. Baboul, B. B. Stefanov, G. Liu, A. Liashenko, P. Piskorz, I. Komaromi, R. Gomperts, R. L. Martin, D. J. Fox, T. Keith, M. A. Al-Laham, C. Y. Peng, A. Nanayakkara, C. Gonzalez, M. Challacombe, P. M. W. Gill, B. G. Johnson, W. Chen, M. W. Wong, J. L. Andres, M. Head-Gordon, E. S. Replogle, J. A. Pople. Gaussian 98 (Revision A.11), Gaussian, Inc., Pittsburgh PA, 2001.
50. C. I. Bayly, P. Cieplak, W. D. Cornell, and P. A. Kollman. A well-behaved electrostatic potential based method using charge restraints for deriving atomic charges: the RESP model. *J. Phys. Chem.* **97**:10269–10280 (1993).
51. P. Cieplak, W. D. Cornell, C. Bayly, and P. A. Kollman. Application of the multimolecule and multiconformational RESP methodology to biopolymers-charge derivation for DNA, RNA, and proteins. *J. Comput. Chem.* **16**:1357–1377 (1995).
52. J. E. Eksterowicz, J. L. Miller, and P. A. Kollman. Calculation of chloroform/water partition coefficients for the N-methylated nucleic acid bases. *J. Phys. Chem. B* **101**:10971–10975 (1997).
53. T.-X. Xiang, B. D. Anderson. Conformational structure, dynamics and solvation free energies of small alanine peptides in water and carbon tetrachloride. *J. Pharm. Sci.* In press. (2005)
54. L. Verlet. Computer "experiments" on classical fluids. I. Thermodynamical properties of Lennard-Jones molecules. *Phys. Rev.* **159**:98–103 (1967).
55. H. J. C. Berendsen, J. P. M. Postma, W. F. van Gunsteren, A. DiNola, and J. R. Haak. Molecular dynamics with coupling to an external bath. *J. Chem. Phys.* **81**:3684–3690 (1984).
56. P. Ewald. Die Berechnung optischer und elektrostatischer Gitterpotentiale. *Ann. Phys.* **64**:253–287 (1921).
57. W. Humphrey, A. Dalke, and K. Schulten. VMD-Visual Molecular Dynamics. *J. Mol. Graph.* **14**:33–38 (1996).
58. T.-X. Xiang. Translational diffusion in lipid bilayers: dynamic free-volume theory and molecular dynamics simulation. *J. Phys. Chem., B* **103**:385–394 (1999).
59. S. H. Glarum. Dielectric relaxation of isoamyl bromide. *J. Chem. Phys.* **33**:639–643 (1960).
60. R. Kohlrausch. Theorie des electrischen Ruckstandes in der Leidner Flasche. *Pogg. Ann. Phys. Chem.* **91**:179–214 (1854).
61. G. Williams and D. C. Watts. Non-symmetrical dielectric relaxation behavior arising from a simple empirical decay function. *Trans. Faraday Soc.* **66**:80–85 (1970).
62. G. Williams, D. C. Watts, S. B. Dev, and A. M. North. Further considerations of non symmetrical dielectric relaxation behaviour arising from a simple empirical decay function. *Trans. Faraday Soc.* **67**:1323–1335 (1971).
63. C. A. Angell. Formation of glasses from liquids and biopolymers. *Science* **267**:1924–1935 (1995).
64. R. G. D. Valle and H. C. Andersen. Molecular dynamics simulation of silica liquid and glass. *J. Chem. Phys.* **97**:2682–2689 (1992).
65. D. T. Turner and A. Schwartz. The glass transition temperature of poly(N-vinylpyrrolidone) by differential scanning calorimetry. *Polymer* **26**:757–762 (1985).
66. T. L. F. Lebedeva, M. Mikhail, A. K. Sergei, and A. Nicolai. A.V. Plate. The products of water H-bonding to poly(N-vinyl pyrrolidone) in solid state. In J. Greve, G. J. Puppels, and C. Otto (eds.), *Spectroscopy of Biological Molecules: New Directions, European Conference on the Spectroscopy of Biological Molecules, 8th* (J. Greve, G.J. Puppels, C. Otto, eds.), Enschede, Netherlands, 1999, pp. 581–582.
67. F. Muller-Plathe. Microscopic dynamics in water-swollen poly (vinyl alcohol). *J. Chem. Phys.* **108**:8252–8263 (1998).
68. F. Franks. Water solubility and sensitivity—hydration effects. In C. A. Finch (ed.), *Chemistry and Technology of Water Soluble Polymers*, Plenum Press, New York, 1981, pp. 157–178.
69. M. J. Chang, A. S. Myerson, and T. K. Kwei. The effect of hydrogen bonding on vapor diffusion in water-soluble polymers. *J. Appl. Polym. Sci.* **66**:279–291 (1997).
70. O. Rodriguez, F. Fornasiero, A. Arce, C. J. Radke, and J. M. Prausnitz. Solubilities and diffusivities of water vapor in poly (methylmethacrylate), poly(2-hydroxyethylmethacrylate), poly(N-vinyl-2-pyrrolidone) and poly(acrylonitrile). *Polymer* **44**:6323–6333 (2003).
71. Y. Wang, G. Meresi, D. Azar, W.-Y. Wen, A. A. Jones, and P. T. Inglefield. Diffusion of decafluropentane in amorphous glassy perflurodioxole copolymer by pulse field NMR spectroscopy. *Macromolecules* **34**:6680–6683 (2001).
72. W. L. C. Vaz and P. F. Almeida. Microscopic *versus* macroscopic diffusion in one-component fluid phase lipid bilayer membranes. *Biophys. J.* **60**:1553–1554 (1991).
73. F. Mueller-Plathe, S. C. Rogers, and W. F. van Gunsteren. Computational evidence for anomalous diffusion of small molecules in amorphous polymers. *Chem. Phys. Lett.* **199**: 237–243 (1992).
74. K. Ichikawa, T. Mori, H. Kitano, M. Fukuda, A. Mochizuki, M. Tanaka. Fourier transform infrared study on the sorption of water to various kinds of polymer thin films. *J. Polym. Sci., B, Polym. Phys.* **39**:2175–2182 (1992).
75. M. H. Cohen and D. Turnbull. Molecular transport in liquids and glasses. *J. Chem. Phys.* **31**:1164–1169 (1959).
76. T.-X. Xiang. A novel dynamic free-volume theory for molecular diffusion in fluids and interphases. *J. Chem. Phys.* **109**: 7876–7884 (1998).